Journal of Oil Palm Research
DOI: https://doi.org/10.21894/jopr.2023.0049

SELECTIVE CYTOTOXICITY EFFECTS OF R-GLYCIDOL AND S-GLYCIDOL ON VERO AND HCT 116 CELLS IN EVALUATING THE INCIDENCE OF GLYCIDYL ESTERS IN EDIBLE OILS AND FATS

SITI NUR SYAHIRAH NOR MAHIRAN[1], NANTHINI A/P RAVI [3], ALAM MAHBOOB [4]* and NURUL HUDA ABD KADIR [1,2]*

ABSTRACT

Despite their feasibility as food flavouring, glycidol is classified as a probable carcinogen under group 2A by WHO. The cytotoxicity effects of isomers of R- and S-glycidol on African green monkey kidney normal cell lines (Vero) and human colon cancer cell line (HCT 116) remain unclear. Cell viability of the treated Vero and HCT 116 cells was determined using the AlamarBlue® assay. Dichlorodihydrofluorescein diacetate (DCFDA) was used to evaluate reactive oxygen species (ROS) activity. Protein expressions of ERK ½, p-ERK, Bcl-2 and caspase-3 were investigated using western blotting technique. The findings indicated that R- and S-glycidol (1.16 µg/mL) exposure dramatically reduced the cell viability of the treated HCT 116 cells but was slightly cytotoxic to Vero cells, hence triggering ROS activity. R- and S-glycidol cause down-regulation of ERK ½, p-ERK, and BCL-2 protein expression at 48 h of treatment. Furthermore, both R- and S-glycidol possess close interaction in proximity to 3D-structure of human ERK and p-ERK protein receptors. In conclusion, R- *and* S-*glycidol potentially triggered oxidative stress and affected ERK protein phosphorylation, leading to caspase-3 independent cell death of the treated HCT 166 cells, suggesting that lower doses (<1.16 µg/mL) of* R- *and* S-*glycidol are safe for human consumption.*

Keywords: cooking oil and lipids, food contaminants, molecular toxicology, safety.

Received: 30 November 2022**; Accepted:** 25 June 2023**; Published online:** 27 September 2023.

INTRODUCTION

Glycidol is widely employed in industrial applications such as the production of sweetening, flavouring compounds, diluent, and dye-levelling agents due to oxiran ring of glycidol that may function as an alkylating agent and contributes to some of its reactivity (Foroumadi and Emami, 2014). Natural oils and vinyl polymers are both produced using glycidol as a stabiliser (Foroumadi and Emami, 2014). Glycidols have become an important key intermediate as substitute dendrimers for the preparation of chemicals, pharmaceuticals, bioactive compounds and food products (Tollini *et al.*, 2022). Mahapatra and Tysoe (2015) have stated that glycidols exist in two stereoisomeric forms, namely, *R*- and *S*-glycidol enantiomers and the difference between the two compounds is only chirality (EFSA Panel on Contaminants in the Food Chain (CONTAM), 2016). Due to biocompatibility with human cells, *R*- and *S*-glycidol have been investigated for their potential as replacement dendrimers for biomedical applications. Dendrimers are hyper-

[1] Faculty of Science and Marine Environment, Universiti Malaysia Terengganu, 21030 Kuala Terengganu, Malaysia.

[2] BIOSES group, Universiti Malaysia Terengganu, 21030 Kuala Terengganu, Malaysia.

[3] Clinical Research, Beacon Hospital, 46050 Petaling Jaya, Selangor, Malaysia.

[4] Division of Chemistry and Biotechnology, Dongguk University, 123 Dongdae-ro, Gyeongju, Republic of Korea.

* *Corresponding author e-mail: nurulhuda@umt.edu.my; mahboobchem@gmail.com*

branched macromolecules which can be functionalised. In order to express explicit biological traits such as lipid bilayer interactions, cytotoxicity, and others, changing their physicochemical properties has made it a suitable delivery vehicle (Abbasi *et al.*, 2014). The benefits of many drugs cannot be exploited because of their poor solubility, toxicity, or stability problems. The use of dendrimers as carriers of bioactive compounds can solve many problems in biomedical approaches and have an advantage in improving their usage for clinical applications (Aurelia *et al.*, 2020). The utilisation of drug combinations based on their targeted administration or drug delivery materials has become a new trend to optimise the therapeutic effects of the drugs with a reduction in adverse effects and potentially becomes a new strategy in the search for successful cancer therapy (Wróbel *et al.*, 2022). In addition, according to a study by Wróbel *et al.* (2022), 2- and 3-poly(amidoamine) (PAMAM G2 and G3) dendrimers covered with *R*-glycidol could penetrate cells faster and exhibited higher toxicity for cancerous cells than for normal cells compared to *S*-glycidol covered analogues. Interestingly, the chirality and functional group of the stereoisomers were reported to alter the physiological of human cells that may contribute to either harmful or harmless effects (Mäder and Kattner, 2020; Moreno-Yruela *et al.*, 2022).

Contradictory, reports by EFSA CONTAM (2016) and Hartwig *et al.* (2020) stated that glycidol is genotoxic (damages DNA) and carcinogenic (causes cancer). The chemicals have the ability to cause adverse effects in rodents (Spungen *et al.*, 2018) that may contribute to genotoxic and mutagenic effects on rats (Bakhiya *et al.*, 2011 and EFSA CONTAM, 2016). Given that the research on glycidol in human is limited, Schilter *et al.* (2011) conducted carcinogenicity bioassays on glycidol in mice and rats in various tissues and found that glycidol induced dose-related increases in the rates of neoplasms. According to Akane *et al.* (2013), adult rats axon injury in the central and peripheral nervous systems were damaged by glycidol, which suggests that it targets the developing nerve terminals of immature granule cells and inhibits late-stage hippocampal neurogenesis. The studies on evaluation of the food contaminant isomers especially the toxicological effect of *R*-glycidol or *S*-glycidol on human cells are limited (EFSA CONTAM, 2016).

Moreover, foods such as infant food formula, margarine, potato crisp, cookies, hot surface cooked pastries, short crusts, fried, roast meat and chocolate spreads were reported to contain harmful food contaminants especially glycidol (EFSA CONTAM, 2016 and Bakhiya *et al.*, 2011). Goh *et al.* (2021) stated that glycidyl esters contamination in palm-based cooking oil were in the range of 1.338 to 18.362 mg/kg. However, the permissible daily glycidol exposure from refined dietary oils and fats is 1.33 g/kg/day (maximum daily fat intake: 80g) for adult individuals weighing 60 kg (Bakhiya *et al.*, 2011). This controversial toxicological effects of glycidols need to be investigated in order to understand underlying mechanism on the safety of the chemical to human normal and cancer cells especially *R*- and *S*-glycidols isomers. Furthermore, limited studies were reported on the genotoxic, mutagenic and cytotoxic effect of glycidols in human normal and cancer cells.

Trans and *cis* fat are example of isomers that have different effects on human cells where *trans*-fat may contribute to carcinogenesis and cancer risk (Matta *et al.*, 2021) but *cis*-fat is considered to be safe to human as it plays important roles as energy source, a component of cellular membranes, and a regulator of different biological process (Hirata, 2021). Despite the fact that the all-trans isomer of astaxanthin (AST) is a potent antioxidant predominates in nature, certain studies have indicated that the cis isomer of AST, particularly the 9-*cis* AST, demonstrated a higher antioxidant potency than the all *trans* isomer (Liu *et al.*, 2016). Furthermore, α-tocopheryl succinate (α-TOS) is selective for cancer cells at least in part due to the lower esterase activity and reduced antioxidant defences expressed by these malignant cells when compared to their normal (non-malignant) counterpart than the others isomers of tocopherols (Constantinou *et al.*, 2008). Lim *et al.* (2014) has suggested that different tocotrienol isomers might exhibit a different cellular mechanism of cell death in different cancer types but specific mechanisms induced by alpha-, gamma- and delta-tocotrienols in both brain and lung cancers are still unclear.

According to Brooks *et al.* (2011) chirality is one of the important factors that plays a role in determining the chemicals interaction with the cancer protein receptors which results in dichotomous effects in normal and cancer human cells. Oxaliplatin isomers of (*R, R*)-cyclohexane-1,2-diamine and (*S, S*)-cyclohexane-1,2-diamine have different roles in inducing cytotoxic effects on leukaemia, lung, colon, breast, renal, melanoma and ovarian human tumour cells. (*S, S*)-cyclohexane-1,2-diamine platinum antineoplastic compound is more biologically active in comparison with (*R, R*)-cyclohexane-1,2-diamine (Arnesano *et al.*, 2015). Toxicological assessment of the glycidol isomers on human cells are limited. Thus, the objectives of this study are to elucidate selective toxicological effects of *R*- and *S*-glycidol in normal and cancer cells. This finding may lead to better understanding of selective cytotoxicity of *R*- and *S*-glycidol in normal cells (monkey) and cancer cells (human), which may be beneficial for safety evaluation of glycidols exposure in food.

MATERIALS AND METHODS

Chemicals

R- and *S*-glycidol were purchased from Sigma Aldrich, USA. RPMI 1640, penicillin-streptomycin and accutase were purchased from Apical Scientific (Gibco, USA). Fetal bovine serum (FBS) was purchased from Apical Scientific (Tico Europe, Netherlands). AlamarBlue® was purchased from Bio-Diagnostics (Invitrogen, Scotland, UK). NucleoSpin® RNA/Protein extraction kit was purchased from Apical Scientific (Macherey-Nagel, Germany). The primary mouse monoclonal ERK ½ (SC-514302), p-ERK (SC-7383), BCL-2 (SC-7382), Caspase (SC-7272) and GAPDH (SC-47724) antibodies were purchased from Santa Cruz Biotechnology (Santa Cruz, CA) and HRP conjugated anti-mouse secondary antibody (A16072) (Life Technologies, USA).

Cell Culture of African Green Monkey Kidney Cell Lines, Vero and HCT 116 Cells

Vero cell line was obtained from Universiti Sultan Zainal Abidin (UNISZA) and HCT 116 cells were obtained from Imperial College London. Vero and HCT 116 cells were maintained in RPMI 1640 media (Gibco, USA), 1% penicillin-streptomycin (Gibco, USA) and 10% FBS (Tico Europe, Netherlands). The flasks were incubated in 37°C humidified incubator supplemented with 5% CO_2. After the cells reached 80%-90% confluency, the cells were trypsinised. The cultures were examined using inverted microscope to check for signs of contamination; old media were discarded. The flasks were rinsed with PBS (3 mL) for three times to discard traces of serum, thereby inhibiting the action of accutase. Accutase (1 mL) was added for trypsinisation process and the flasks were incubated at 3°C and 5% humidified incubator for 5 min to detach the cells. Complete medium (3 mL) was added, and the solutions were transferred into 15 mL centrifuge tubes before spinning down at 2500 rpm for 5 min. The supernatants were discarded, and the pellet of Vero and HCT 116 cell lines was used for the next procedure. The cells and media (10 µL) were transferred immediately to the edge of the hemocytometer chamber, and the slide was viewed under inverted microscope. The cells were counted within the four corners of the grid. Non-viable cells were stained blue (Kim *et al.*, 2016).

The final volume of fresh media and treatment solution (1 µL) was 100 µL in each plate. The 96-well plate that contains 99 µL of seeded cells and fresh complete medium was incubated overnight in 37°C humidified incubator supplemented with 5% CO_2 (Kadir *et al.*, 2009).

AlamarBlue® Assay by Using Vero and HCT 116 Cell Lines

Different concentrations of *R*- and *S*-glycidol (0.000116 µg/mL, 0.00116 µg/mL, 0.0116 µg/mL, 0.116 µg/mL and 1.16 µg/mL) were used to treat the Vero and HCT 116 cell lines. Four replicates of the treatment were conducted on 96-well plates and incubated in 37°C humidified incubator supplemented with 5% CO_2 for 24, 48 and 72 hr. AlamarBlue® reagent (10 µL was added into each well and immediately incubated back in the same condition for 4 hr. Resazurin (opaque blue) in AlamarBlue® reagent was converted to resorufin (fluorescence pink) via the reduction reactions of metabolically active cells. The absorbance values were measured at 570 nm excitation wavelength value and 590 nm emission wavelength value by using microplate reader (Thermo Fisher Scientific, USA) (Bonnier *et al.*, 2015).

ROS by Using 2,7-dichlorofluorescin Diacetate (DCFDA) Dye

The cells were seeded in 24-well plate, and 1×10^5 cells were seeded in each well. The 24-well plates containing cells were incubated overnight. Dichlorodihydrofluorescein diacetate (DCFDA) powder (Sigma Aldrich, USA) was used to measure ROS activity in treated HCT 116 cells. 5 mg of DCFDA was mixed with dimethylsulfoxide (DMSO) (4.104 mL). DCFDA (2.5 µL) was added to the wells containing cells and incubated in an incubator for 30 min. After 30 min, the medium in each well was discarded carefully and washed with PBS. The media were added in each well and treated with different concentrations of *R*- and *S*-glycidol. 5 µL of the treatment solutions was aliquoted in media containing HCT 116 cells (500 µL) that were pre-treated with DCFDA. The treated cells were immediately incubated at 37°C with 5% CO_2. The samples were measured for every 1 hr by using microplate reader. The absorbance values were measured fluorometrically at excitation of 520 nm and emission of 550 nm (Wu and Yotnda, 2015).

Protein Extraction

2.5×10^5 of HCT 116 cells were seeded in six-well plate and treated with 500 mM to obtain final concentration of 5 mM for 24 and 48 hr. The seeded cells that were treated with 0.01% DMSO was used as a negative control for both time points. The cells were incubated for 24 and 48 hr prior to treatment with *R*-glycidol and *S*-glycidol and trypsinisation. The cell pellets were washed with 3 mL PBS and centrifuged at 3000 rpm for 5 min. The supernatants were completely discarded by pipetting, and the pellets were stored in −80°C until the next procedure

was conducted. Proteins from the samples of treated cells were extracted using NucleoSpin® RNA/ Protein (Macherey-Nagel) protocol with slight modifications. Bradford assay was performed using Bio-Rad Protein Assay (Bio-Rad, USA) to determine protein concentrations. The absorbance of the samples was measured at 595 nm by using ELISA plate reader (Bio-Rad, USA) (Sinkala *et al.*, 2017).

Western Blotting, Blocking and Gel Dot

Loading samples of the treated HCT 116 cells with *R*- and *S*-glycidol were prepared according to manufacturer's instructions (Pub. Part No. IM-8042). 20.0 µg/µL protein samples, 3.75 µL NuPAGE® LDS sample buffer (4X), 0.75 µL BME and deionised water were mixed together with the total volume of 15 µL. The mixture was heated at 72°C for 10 min at 500 rpm. 1X SDS running buffer was poured in XCell SureLock™ Mini-Cell electrophoresis tank. Protein samples (15 µL) from section 2.5 were loaded in NuPAGE 4%-12% Bris-Tris gel (Novex, Life Technologies, USA) by using loading tips. The system was run at voltage 200 V and 100-125 mA for 1 hr and 30 min. After that, the gel was taken out from its cassette and washed three times with ultrapure water. The SDS-PAGE gel was then stained with SimplyBlue® safe stain for 2 hr. The gel was destained by ultrapure water overnight. The image was observed by using gel imager (Gel Doc XR + system, Bio-Rad, USA). After separating the protein mixture, it was transferred to a PVDF membrane.

The PVDF membrane was soaked in a blocking buffer (5% of non-fat dry milk) for 2 hr. The membrane was incubated overnight with primary mouse monoclonal ERK ½ at 4ºC. Subsequently, the membrane was incubated with HRP conjugated anti-mouse secondary antibody (1:2200 dilution) for 4 hr. The membrane was washed with Tris-buffered saline with Tween 20 (TBST) buffer (20 mM Tris pH 7.5, 150 mM NaCl, 0.1% Tween 20) for three times. The bounded antibody was detected by using chromogenic peroxidase substrate (Life technologies, USA). Gel dot was used to measure band intensity. The image was analysed by using ImageJ software.

Then, the membrane was washed with TBST for 3 hr before it was soaked with other antibody and blocking buffer (5% of non-fat dry milk) for 2 hr. The same step was repeated for another antibody, namely, p-ERK (1:1000 dilution), BCL-2 (1:1000 dilution), Caspase-3 (1:1000 dilution), GAPDH (1:5000 dilution). Whereas, GAPDH protein expression was used as loading controls.

Molecular Docking Study

AutoDock 4.2 and AutoDock Tools (Morris *et al.*, 2009) were used to examine the nonbonding interaction of the 3D-structure of human ERK2 (PDB: 4FMQ) and Phosphorylated Map Kinase ERK2 (PDB: 2ERK) with *R*- and *S*-glycidol through molecular docking study (Aral *et al.*, 2012). The crystal structures were downloaded from the RCSB PDB and prepared for molecular docking in two steps. The protein data bank (PDB) files (4FMQ and 2ERK) were separately imported into AutoDock Tools (ADT), the graphical user interface for AutoDock, as the first step. Water molecules, ligands, and any associated molecules were removed from the receptor (protein) structure (PDB: 4FMQ and 2ERK) during this process. Next, the receptor was prepared by adding missing hydrogen atoms, residues, and charges. The *R*- and *S*-glycidol structure were retrieved from PubChem and the energy of the molecules was minimised for optimal geometrical parameters for docking with AutoDock 4.2. The best dock poses obtained from docking simulations were used for visualisation using Discovery Studio software (BIOVIA Discovery Studio 2016).

Statistical Analysis

GraphPad Prism V was used to analyse cell viability, ROS level and western blot analysis value. One-way ANOVA analysis with Dunnet post-test and two-way ANOVA with Bonferroni multiple comparison test were used to determine significant difference of cell viability and ROS at $p<0.05$ of the treated HCT 116 with *R*- and *S*-glycidol. However, unpaired t-test was used to determine significant difference of protein expression in the treated human colon, HCT 116 cell lines.

RESULTS

Cytotoxicity Effect of *R*- and *S*-glycidol on Vero and HCT 116 Cell Lines

In order to determine the toxicity of *R*- and *S*-glycidol, Alamar blue was performed on normal and cancer cell lines. *Figure 1 [i(a)]; [ii(a)]; [iii(a)]; [i(b)]; [ii(b)]* and *[iii(b)]* shows percentage cell viability of Vero and HCT 116 after treatment with *R*-glycidol and *S*-glycidol. Based on our result, *R*- and *S*-glycidol caused the inhibition of cell viability at 24, 48 and 72 hr of the treatment for HCT 116 but not for the Vero cells. *R*- and *S*-glycidol showed a slight cytotoxicity effect on Vero cells persistent with the increased time points. However, the inhibition activity of treated HCT 116 cells were more cytotoxic and prominent when the cells were exposed to *R*- and *S*-glycidol at higher dose and time of the exposure, suggesting that the cytotoxicity effect were dose and time dependent. This interesting results on cell viability of the treated Vero and HCT 116 cells has proven the selectivity on cytotoxicity effects of *R*- and *S*-glycidol exposure. Based on our findings, 50%

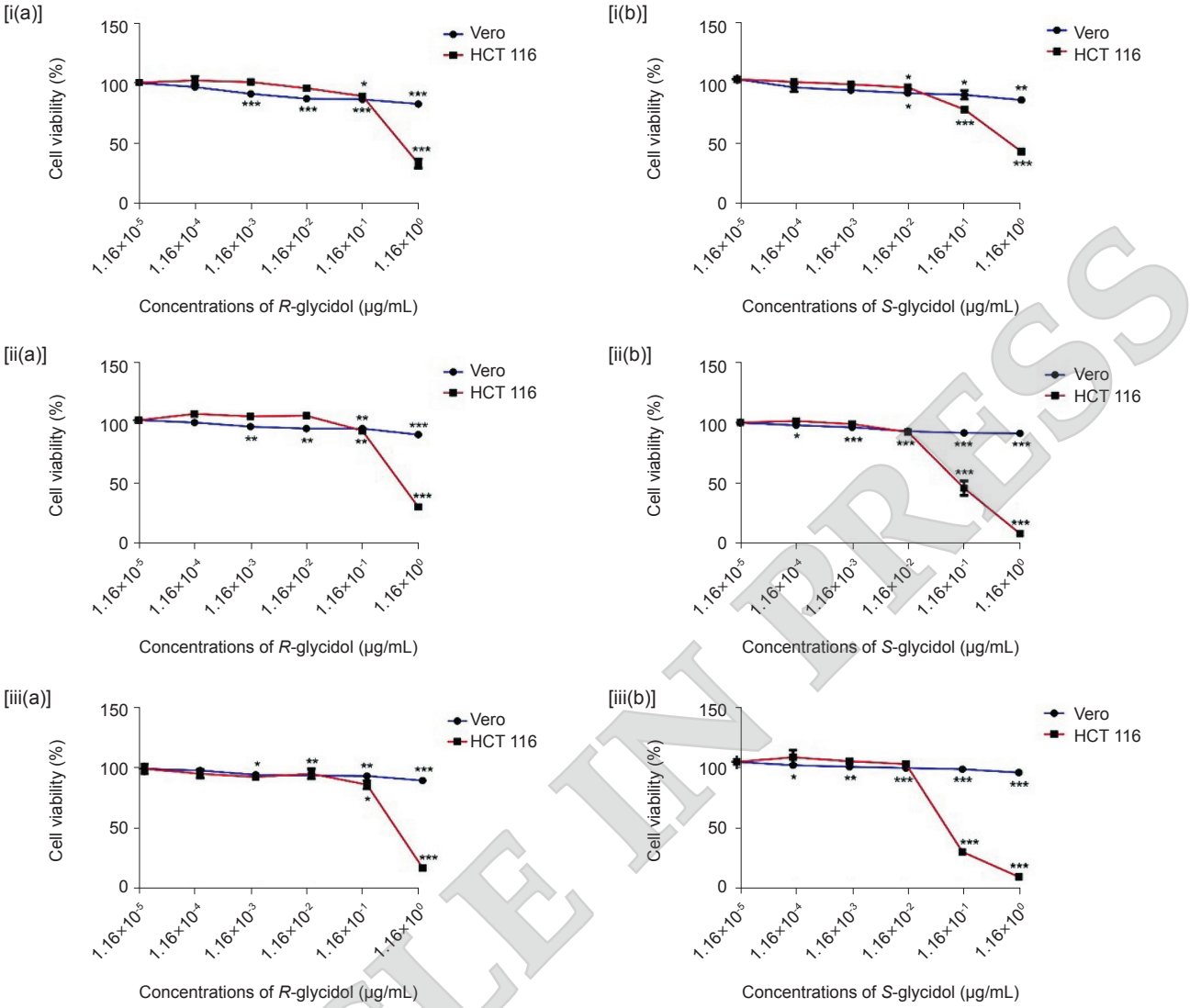

Figure 1. Cytotoxicity effect of Vero and HCT 116 cells after 24 (1), 48 (2) and 72 (3) hr of treatment with R*-glycidol (a) and* S*-glycidol (b). The analysis was performed using GraphPad Prism V and one-way ANOVA analysis with Dunnet post-test were done. * indicates* $p<0.05$*, ** indicates* $p<0.01$*, *** indicates* $p<0.001$ *significant difference of the concentration towards the control.*

of inhibition concentration (IC_{50}) values *R*-glycidol of the treated HCT 116 cells were 5.0, 4.5 and 3.4 µg/mL at 24, 48 and 72 hr of treatment, respectively. Whereas IC_{50} values of the treated HCT 116 cells with *S*-glycidol were 4.8, 0.7 and 0.4 µg/mL at 24, 48 and 72 hr of treatment, respectively. Interestingly, the exposure of *R*- and *S*-glycidol on Vero cells did not exceed 50% of cell inhibition indicating that the chemicals were less toxic to normal cells. Moreover, the cell cytotoxicity effects of both chemicals have shown similar trend of cells inhibition, suggesting that the isomers of glycidols did not contribute much on the cytotoxic effects.

Reactive Oxygen Species (ROS) Expression

In ROS level was determined to evaluate the oxidative stress event after the exposure *R*- and *S*-glycidol on HCT 116 cells. *Figure 2a* shows significant increase at concentration of 10 mM of the treatments compared to control at time points 6 and 24 hr, but other concentrations of *R*- and *S*-glycidol treatments had negligible effect. The data suggested that the highest concentration of *R*-glycidol (1.16 µg/mL) exposure resulted in significant increase in ROS level of the treated HCT 116 cells, whereas other concentrations of the treatment showed slight increase in ROS level of the treated HCT 116 cells with *R*- and *S*-glycidol, suggesting that oxidative stress was expressed after the exposure of *R*-glycidol to HCT 116 cells at 24 hr. *Figure 2b* shows significant increase in ROS production after the treatment with *S*-glycidol (1.16 µg/mL) compared to control. However, other concentrations of the treatments showed negligible effect. The data suggested that the highest concentration of *R*- and *S*-glycidol may

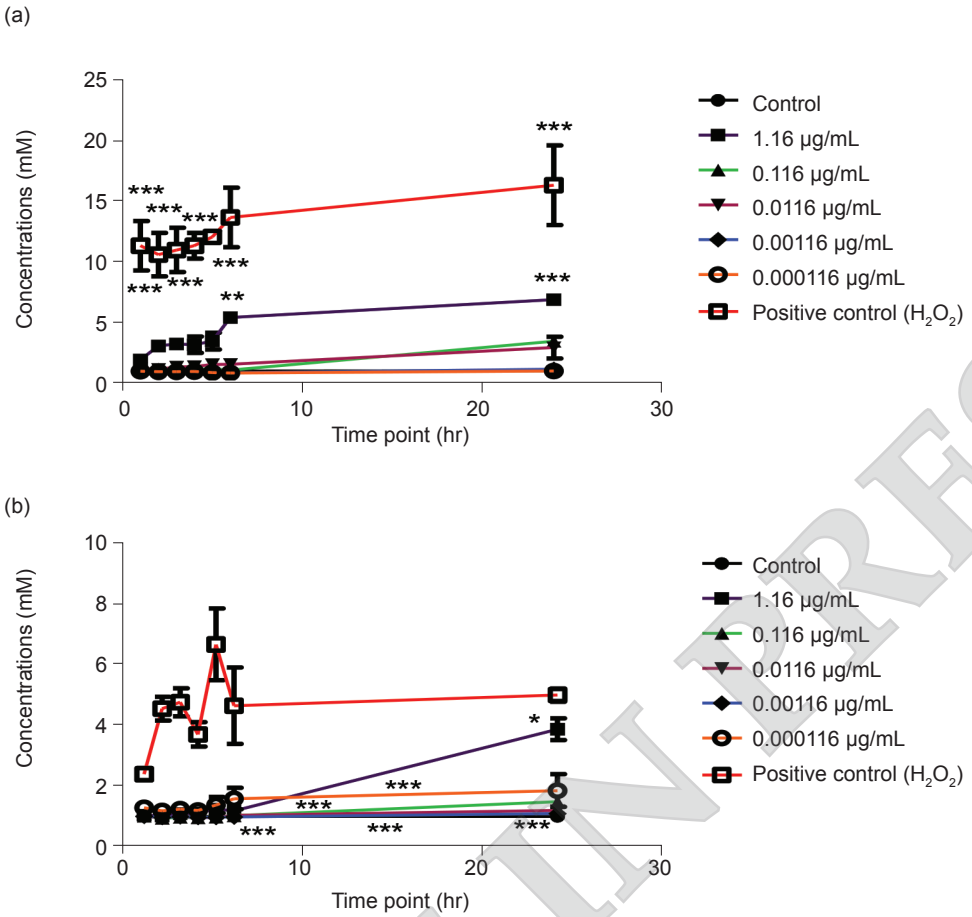

Figure 2. ROS expression of HCT 116 cells after 24 hr treatment of (a) R*-glycidol, and (b)* S*-glycidol. Two-way ANOVA with Bonferroni multiple comparison test were done and * indicates* $p<0.05$, ** *indicates* $p<0.01$, *** *indicates* $p<0.001$ *significant difference of the concentration towards the control.*

induce significant increase in ROS level of the treated HCT 116 cells. Whilst, the other concentrations of the treatment of both chemicals showed slight increase in ROS level in the treated HCT 116 cells, suggesting that oxidative stress was expressed after the exposure of *R*- and *S*-glycidol. We speculated that oxidative stress might be the main cause of the cytotoxic effect in the HCT 116 cells after the exposure with *R*- and *S*-glycidol.

Western Blot Analysis of the Protein Expressions

ERK ½ is a protein in MAPK pathway that may contribute to oxidative stress event in cells. Furthermore, the expression of ERK ½ protein (42 kD), p-ERK protein (43-55 kD), BCL-2 protein (26 kD), Caspase-3 (35 kD) and GAPDH (36 kD) using western blotting technique were done to elucidate the mechanism in the cells. The expression of ERK ½ protein (42 kD), p-ERK protein (43-55 kD), BCL-2 protein (26 kD), Caspase-3 (35 kD) and GAPDH (36 kD) expression of the treated HCT 116 cells with *R*- and *S*-glycidol at 24- and 48-hr treatments are shown in *Figure 3a* and *3b*, respectively. Protein bands were intensely expressed on the PVDF membrane of the treated HCT 116 cells with *R*- and *S*-glycidol (1.16 µg/mL) compared to control at 24 and 48 hr of the exposure.

As shown in *Figure 3c*, there was no significant difference between the ERK ½ protein expression of the treated HCT 116 cells with *R*-glycidol compared to control after 24 hr of the treatment. However, after 48 hr of exposure, HCT 116 treated with *R*-glycidol showed a marginal decrease compared to control with significant difference at $p<0.05$. On the other hand, *S*-glycidol exposure to HCT 116 cells showed significant down regulation ($p<0.01$) at 48 hr exposure of the ERK ½ protein expression, but the expression of ERK ½ protein at 24 hr showed no significant difference, suggesting that the expression of ERK ½ protein of *R*- and *S*-glycidol treatments in HCT 116 cells took longer time of exposure to show the effect. The p-ERK protein expression of the treated HCT 116 cells with *R*- and *S*-glycidol showed no significant difference compared to control at 24 hr treatment, but at 48 hr treatment, it showed significant decrease ($p<0.01$) (as shown in *Figure 3d*). Interestingly, BCL-2 protein expression

in *Figure 3e* was down-regulated compared with the control with significant difference of $p<0.05$ at 48 hr but no significance at 24 hr after *R*- and *S*-glycidol exposure. This finding suggested that pro-apoptotic event might occur during 48 hr of the exposure. However, caspase-3 protein expression of the HCT 116 cells showed no significant difference compared to control after the treatment with free *R*-glycidol at 24 hr and 48 hr (*Figure 3f*). Whereas caspase-3 protein expression of the treated HCT 116 cells with free *S*-glycidol was significantly down-regulated ($p<0.001$) compared to the control at 48 hr of exposure but no significance at 24 hr of *S*-glycidol exposure. This finding suggested that cell death induced by *R*-glycidol was caspase-3 independent.

Relative density ratio of p-ERK and ERK ½ and proteins was calculated to assess the phosphorylation event of ERK. The results in *Figure 4a* and *4b* indicate that the relative density ratio p-ERK/ERK ½ of the HCT 116 cells treated with *R*-glycidol was significantly lower than the control at 48 hr of exposure but not significant at 24 hr of exposure. Meanwhile, relative density ratio p-ERK/ERK ½ of the HCT 116 cells treated with *S*-glycidol *(Figure 4c* and *4d)* showed no significant difference at both 24 and 48 hr of the exposure. The findings suggest that the cytotoxicity and oxidative stress in the treated cells with *R*-glycidol were likely due to phosphorylation event of ERK protein.

Molecular Docking Analysis

In silico study was conducted to support protein expression data, and the molecular docking result showed an interaction between *R*- and *S*-glycidol *(Figure 5(c,d); Figure 6(c,d))* and ERK2 *(Figure 5a)* and phosphorylated Map Kinase ERK2 *(Figure 6a)* protein receptor. A molecular docking simulation involving two receptors (PDB: 4FMQ and 2ERK) and two compounds (*R*- and *S*-glycidol) was performed using AutoDock 4.2. The top four docking poses in this simulation were selected based on their binding energies, which ranged from -3.42 to -4.0 kcal/mol. These selected poses were further investigated in Discovery Studio to investigate the interactions of *R*- and *S*-glycidol with the 3D structures of the human ERK2 protein (PDB: 4FMQ) and pERK2 (PDB: 2ERK). The results are shown in *Figure 5* and *6*. In *Figure 5(d,e)*, the active amino acid residues form a cavity that resembles a sphere around the molecule. The presence of glycidol is close to the hydrophobic and hydrophilic radicals, leading to different secondary forces, such as Van der Waals contacts and hydrogen bonding. This hydrophobic contact, hydrogen bonding and Van der Waals forces contribute in the binding interaction between chemical compounds and active amino residues of the receptor. *R*- and *S*-glycidol formed two hydrogen bonds with MET108 and ASP106 with distances of 1.62276-2.30747 Å, as well as Van der Waals contacts with the amino acid residues LEU017, ALA52, LEU156, ILE84 and GLN105 as represented in *Figures 5 (h, i)*. These binding interactions allow the drug to connect closely with the receptor, inhibiting the activity of the cells in the system. The hydrophobic receptor residues involved in interactions with compounds, such as LEU, ILE, and ALA, as well as the hydrophilic amino acid GLN, provide extra strength inside the active pocket. This condition allows for a better mutual relationship between the ligand and the receptor, paving the way for inhibitory drug development. The binding details and bond lengths achieved through molecular docking are shown in *Table 1*. Docking analysis *(Table 1)* revealed that *R*- and *S*-glycidol interacted with the protein in the best possible orientation to stabilise the structures by making close contact with the receptor cavities. As a result, at their best docked positions, both compounds exhibit similar interactions and approximately similar binding energies, culminating in similar inhibition activities in experimental studies for both compounds (*R*- and *S*-glycidol).

DISCUSSION

A study by Abraham *et al.* (2011), indicated that different isomers may provide different effects, and the induction mechanism in human cells should be studied. Two enantiomers from same chemical composition that has different chirality could react differently in biochemical process or biological reaction of cells (Fanali *et al.*, 2019). At the low concentration less than 5 μg/mL of glycidol, it did not show any toxicity effects on Chinese hamster ovary (CHO) cells as the cell toxicity treated with glycidol never exceeded more than 8% in CHO as measured by trypan blue dye exclusion (El Ramy *et al.*, 2007). Based on our findings, IC_{50} values of cell viability of treated HCT 116 cells with *R*- and *S*-glycidol at 24, 48 and 72 hr were 5.0, 4.5, 3.4 μg/mL and 4.8, 0.7, 0.4 μg/mL, respectively. This result has shown that the cytotoxicity effect of both glycidols are dose and time dependant. Our finding is supported by Senyildiz *et al.* (2017), who stated that cytotoxicity of glycidols and 3-MCPD were dose and time dependant. Ozcagli *et al.* (2016) found that 3-MCPD, glycidol and β-chlorolactic acid also reduced the cell viability of human embryonic kidney cells (HEK-293) and kidney epithelial cell lines (NRK-52E) at 24 hr treatment by using MTT assay. Furthermore, Liu *et al.* (2021) indicated that glycidol at different doses of treatments using NRK-52E cells induced a significant cytotoxicity effect in a dose and time dependent.

The glycidol induce ROS by damaging DNA and proteins in the cells as the epoxide group of the

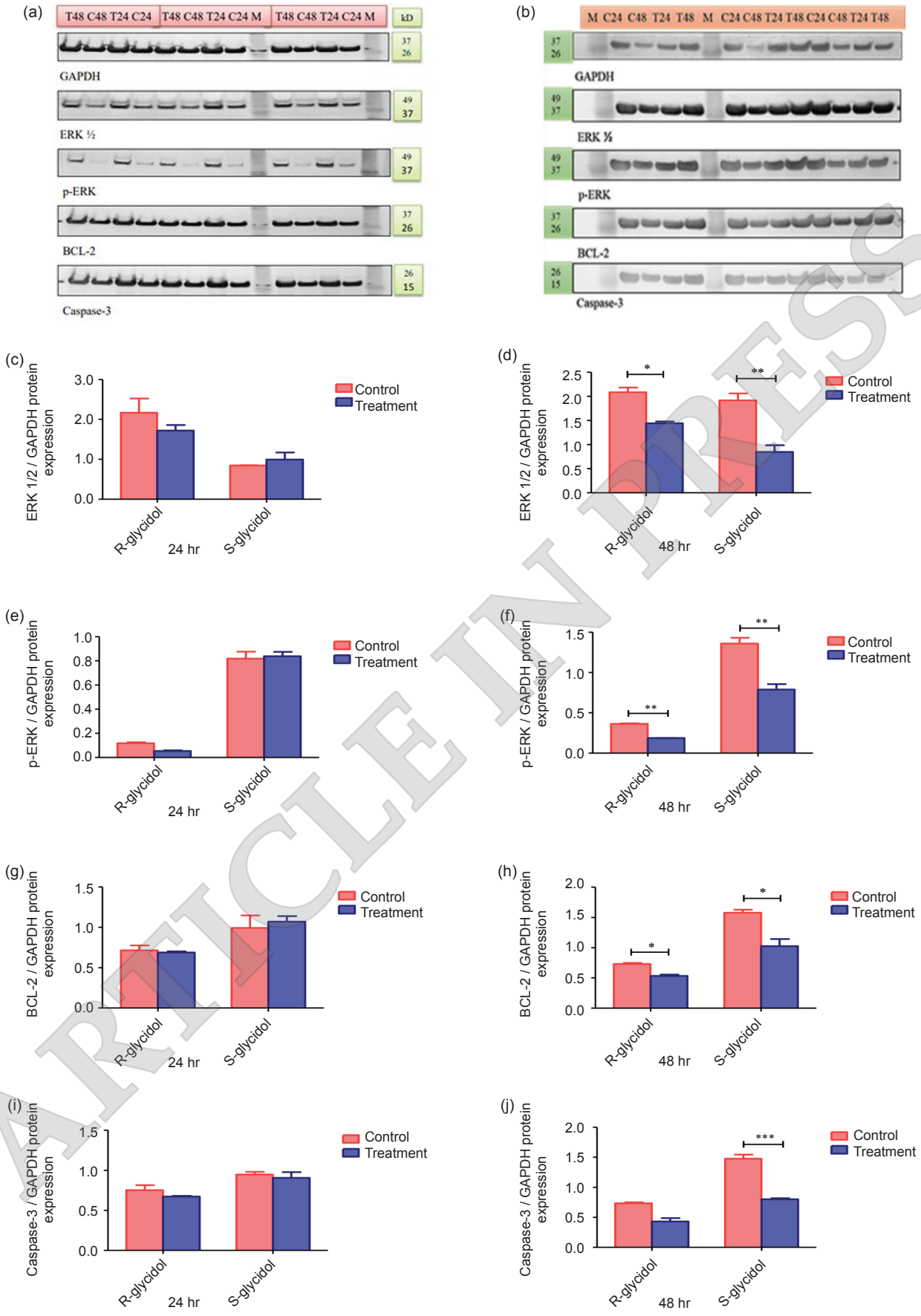

Figure 3. (a) R-*glycidol, and (b)* S-*glycidol protein bands of targeted protein located between 15 kD and 49 kD on PVDF membrane using western blot technique. (M) protein marker; (C24) Control 24 hr; (T24) IC_{50} 24 hr; (C48) Control 48 hr; (T48) IC_{50} 48 hr. Intensity area (c, d, e and f) of the targeted protein mitogen-activated protein kinase of* R- *and* S-*glycidol at 24 and 48 hr. The analysis was done by using ImageJ software.*

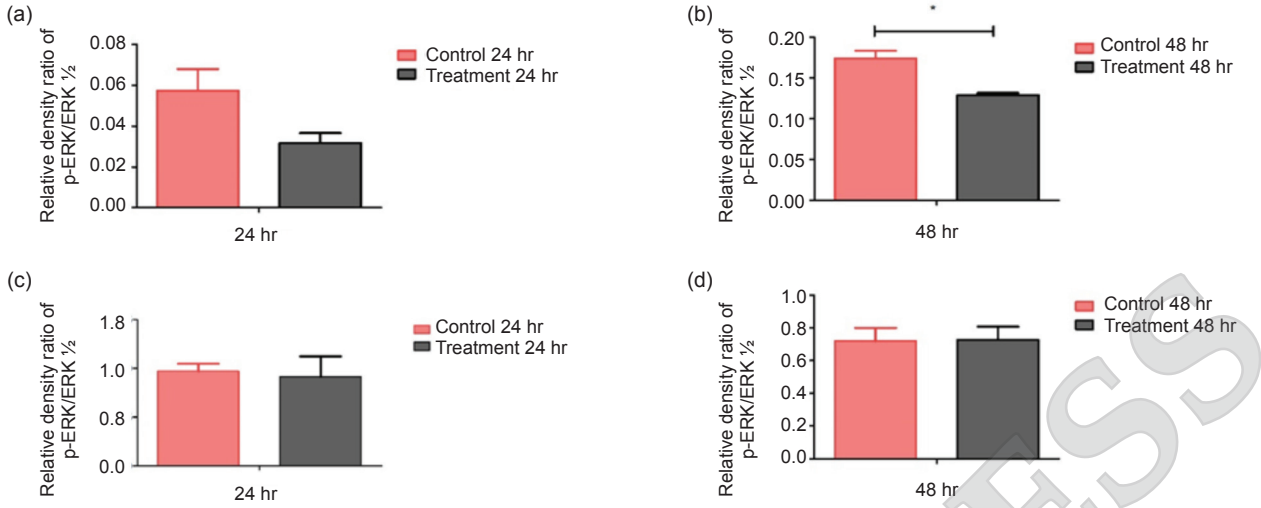

Figure 4. Relative density ratio of p-ERK/ERK ½ proteins of the treated HCT 116 cells with R-*glycidol (a and b) and* S-*glycidol (c and d) at 24 and 48 hr treatments, respectively.*

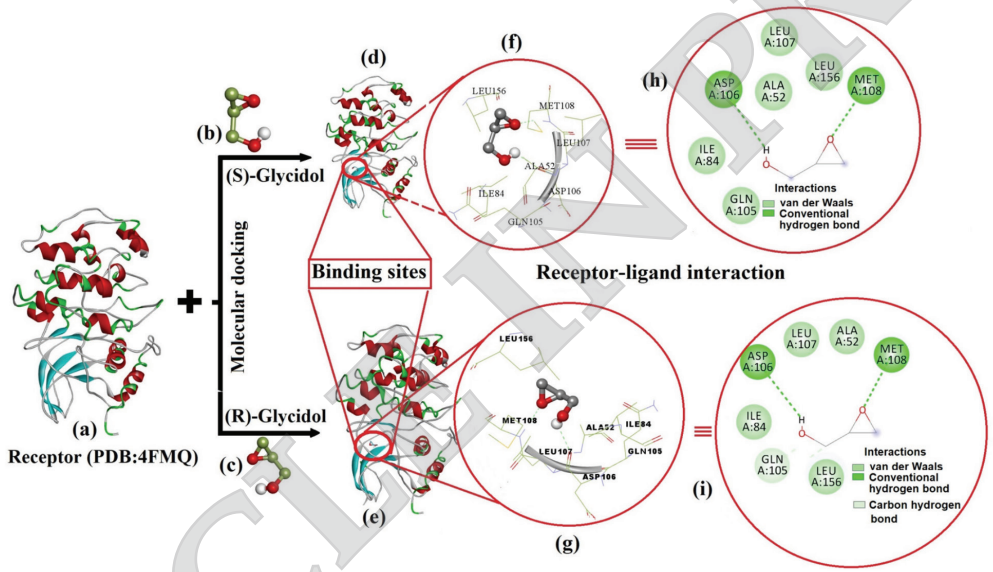

Figure 5. Molecular docking study of (a) human ERK2 (b, c) S- *and* R-*glycidol, (d, e) active pocket of receptor shown by sphere around compounds, (f, g) involvement of various hydrophobic amino acids including a hydrophilic amino acid with the studied compounds, and (h, i) 2D representation for the buried compound inside cavity of receptor showing hydrogen bond, van der Waals, and other secondary forces.*

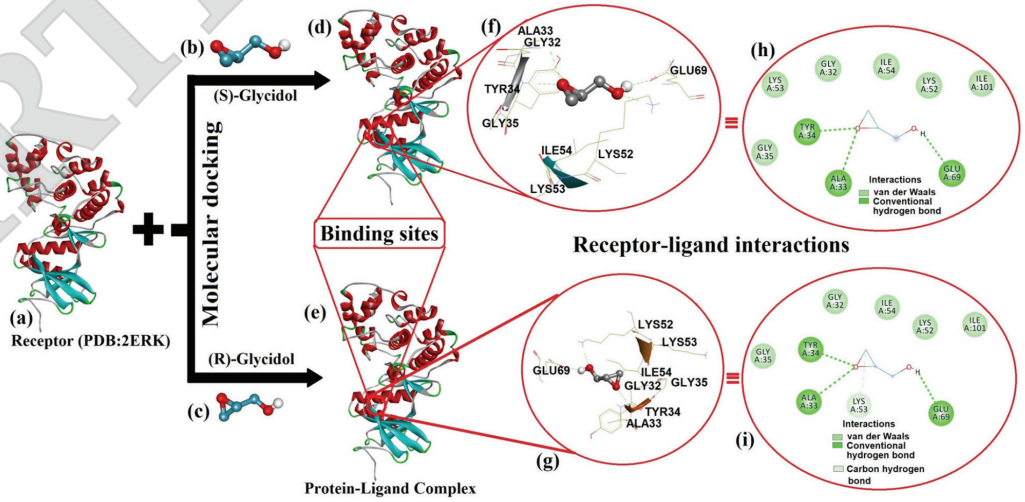

Figure 6. Molecular docking study of (a) Phosphorylated Map Kinase ERK2 (b, c) S- *and* R-*glycidol, (d, e) active pocket of receptor shown by sphere around compounds, (f, g) involvement of various hydrophobic amino acids including a hydrophilic amino acid with the studied compounds, and (h, i) 2D representation for the buried compound inside cavity of receptor showing hydrogen bond, van der Waals, and other secondary forces.*

TABLE 1. THE BINDING OF *R*- AND S-GLYCIDOL WITH RECEPTORS (PDB: 4FMQ AND 2ERK) RESULTED FROM MOLECULAR DOCKING WITH THEIR MODE OF BINDING

Receptor	*R*-glycidol		*S*-glycidol	
	HB Distance (A°)	Nature of interaction	HB Distance (A°)	Nature of interaction
Human ERK2 complexed with a MAPK (PDB: 4FMQ)	1.64289 2.21280	MET108:R-Lig (HB) S-Lig:ASP106 (HB) LEU107-R-Lig (vdW) LEU156-R-Lig (vdW) ALA52-R-Lig (vdW) ILE84-R-Lig (vdW) GLN105-R-Lig (CHB)	1.62276 2.08040	MET108:S-Lig (HB) S-Lig:ASP106 (HB) LEU107-S-Lig (vdW) LEU156-S-Lig (vdW) ALA52-S-Lig (vdW) ILE84-S-Lig (vdW) GLN105-S-Lig (vdW)
Phosphorylate-Map Kinase ERK2 (PDB:2ERK)	1.89862 1.77878 1.94482	TYR34:R-Lig (HB) ALA33:R-Lig (HB) R-Lig:GLU69 (HB) GLY35-R-Lig (vdW) GLY32-R-Lig (vdW) ILE54-R-Lig (vdW) LYS52-R-Lig (vdW) LYS53-R-Lig (CHB)	1.96735 2.40056 1.88987	TYR34:S-Lig (HB) ALA33:S-Lig (HB) S-Lig:GLU69 (HB) GLY35-S-Lig (vdW) GLY32-S-Lig (vdW) ILE54-S-Lig (vdW) LYS52-S-Lig (vdW) LYS53-S-Lig (vdW)

Note: HD-hydrogen bond; vdW-Van der Waals forces; CHB-carbon hydrogen bond; S-Lig-*S*-glycidol; R-Lig-*S*-glycidol.

glycidol may react with the macromolecules in the cells (Sevim *et al.*, 2021). The epoxide group of the glycidol have the ability to react with the nucleophilic biomolecules such as protein in the cells that may triggers ROS production (Inagaki *et al.*, 2019). ROS level of treated 116 cells with *R*- and *S*-glycidol *(Figure 2)* had shown that both chemicals are able to induce oxidative stress. This may be due to ROS levels have been found to be elevated in almost all cancers, promoting several aspects of tumour formation and progression (Liou and Storz, 2010). The increase in ROS production (oxidative stress) might mediate changes in the biological response that cause cell and tissue damage (NavaneethaKrishnan *et al.*, 2019; Pizzino *et al.*, 2017; Snezhkina *et al.*, 2019). In addition, the oxidative stress event may cause the induction of mitochondrial cytochrome C which triggered by the ROS (Ji *et al.*, 2017). Our results also supported by Mossoba *et al.* (2020) who reported that HK-2 cells that were treated with 3-MCPD and its esters have shown slightly increased in ROS levels with the increasing concentrations of the treatment. ROS are a typical by product of oxidative energy metabolism and are thought to have a role in various intracellular signalling pathways, including the MAPK pathway (Rezatabar *et al.*, 2019). According to Circu and Aw (2010), concentrations of compound are the most important factors that affect ROS production because it is a product of normal metabolism during xenobiotic exposure. Increasing ROS production can occur when mutation in mitochondrial genes is observed (Redza-Dutordoir and Averill-Bates, 2016). The formation of superoxide can occur when the electron transfer is inhibited along the electron transport chain (ETC). Thus, this radical yielding hydrogen peroxide (H_2O_2) by diffusion into cell nucleus and DNA attack leads to the genetic instability (Schumacker, 2006). At low level, ROS can function as redox messenger in most intracellular signalling. Otherwise, excessive or high production of ROS would induce oxidative stress of cellular macromolecules that might inhibit protein function and promote cell death that could lead to DNA damage, apoptosis and cancer development (Fu *et al.*, 2014).

The results in *Figure 3* showed that high concentration of *R*- and *S*-glycidol compound affected protein expressions of ERK ½, p-ERK, BCL-2 and caspase-3. This effect was due to phosphorylation event of ERK ½ that might be responsible in inducing oxidative stress and further led to cell death (Liou and Storz, 2010). Furthermore, docking results *(Figure 5* and *6)* shows that *R*- and *S*-glycidol have similar interactions and relatively similar binding energies, resulting in similar inhibition activities of ERK ½, p-ERK proteins after the treatment with both compounds. We speculated that the down regulation of ERK ½ and p-ERK protein expression for HCT 116 cells treated with both *R*- and *S*-glycidol might activate the phosphorylation event of ERK protein *(Figure 4)* when ROS is elevated *(Figure 2),* thereby leading to oxidative stress that may contribute to cytotoxic effect. The cell death mechanism of *R*- and *S*-glycidol is shown in *Figure 7.* As in human cells, the Raf/MEK/ERK module was activated through MAPK pathway as shown in *Figure 7*. *R*- and *S*-glycidol potentially induce the production of ROS by triggering the MAPK pathway that involves ERK ½, p-ERK, BCL-2 and caspase-3. In the nucleus, DNA alteration occur as the phosphorylated ERK and BCL-2 were activated that might lead to the DNA damage and cell death. ERK ½ requires simultaneous

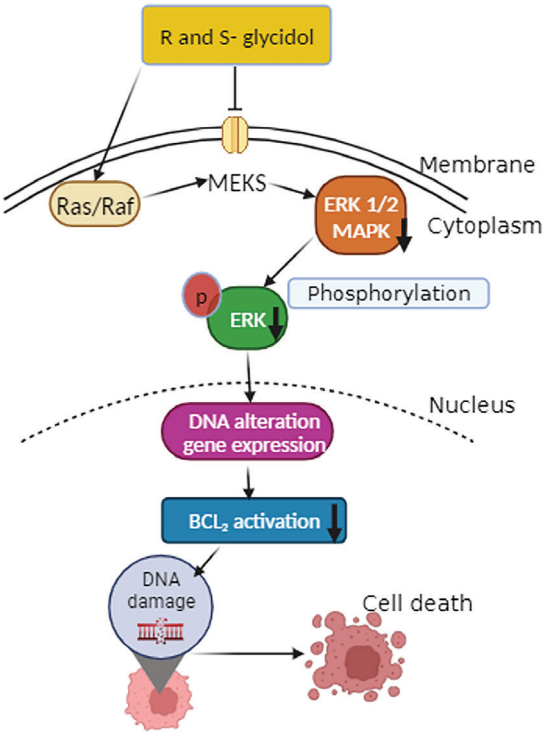

Figure 7. Schematic diagram of cell death mechanism after treatment with R- *and* S-*glycidol in HCT 116 cells.*

phosphorylation at conserved threonine (Thr) and tyrosine (Tyr) residues to be fully activated. As the result of the phosphorylation event, the ERK ½ kinase protein undergoes conformational changes, domain rotation and remodelling which allowing substrates to bind and be phosphorylated by ERK ½ kinase (Takahashi *et al.*, 2012).

Caspase-mediated intrinsic signalling system, which is mostly regulated by the BCL-2 family of intracellular proteins, or an extrinsic signalling pathway, which is primarily regulated by the tumour necrosis factor (TNF) receptor family, can both cause apoptosis (Lu *et al.*, 2020). Apoptosis dysregulation is linked to uncontrolled cell proliferation, cell growth, and cancer development (Takahashi *et al.*, 2012). Based on our findings, BCL-2 protein expression for both *R*- and *S*-glycidol were down regulated as the time exposure increased *(Figure 3)*. We postulated that the down regulation of BCL 2 contributes to cell death of treated HCT 116 cells after *R*- and *S*-glycidol treatments. According to Ji *et al.* (2017), the decreasing BCL-2 protein expression after exposure of 3-MCPD resulted in activation of mitochondrial apoptosis pathway. In order to prove whether early apoptotic event occurred or not, caspase-3 protein expression was conducted and caspase-3 protein expression showed no significant difference compared to control after treated with *R*- and *S*-glycidol in the HCT 116 cells *(Figure 3)*. This event suggested that induction of cell death by *R*- and *S*-glycidol in the treated HCT 116 cells was caspase independent. A study by Kim *et al.* (2021), indicated that cytotoxic effects on human lung cells after treated with mercury chloride ($HgCl_2$), subsequently leading to the cell death via caspase-3 independent pathway. Previous studies also indicated that cell death event in various types of cells (*in vitro)* which mediated cell death via caspase-3 independent (Cregan *et al.*, 2013; Mallepogu *et al.*, 2017; Nowak *et al.*, 2020). In addition, glycidol has an ability to induce immunoreactivity which may lead to the apoptosis in the Albino rat brain cells (Sevim *et al.*, 2021). Furthermore, epoxide functional group in the chemical structure of metabolites (chemicals undergo xenobiotic metabolism) has high reactivity that was proven to promote high toxicity than the parent compound (Obach and Kalgutkar, 2010). The epoxide of the glycidol was believed the cause of DNA damage in human cells that mediated cell death (Liu *et al.*, 2021). The free glycidol was discovered to induce cell cycle arrest and apoptosis event with the involvement MAPK. RAS/RAF/MEK/ERK proteins are proteins in MAPK pathway, which are the most common proteins in cancer cell biology especially in oxidative stress event of the cancer cells (De Luca *et al.*, 2012). McCubrey *et al.* (2012), reported that activated ERK ½ S/T kinases phosphorylated and activated various substrates, and this pathway was involved in cancer development. Furthermore, ERK MAPK overexpression and activation have a role in the proliferation and progression of cancer cells development (Fang and Richardson, 2005). RAS protein or originally known as Rat Sarcoma Virus (RAS) protein can be found in human. The RAS protein mediates the ERK pathway, which subsequently activates rapidly accelerated fibrosarcoma 1 (RAF1), triggering a cascade involving MEK and then ERK activation, which was involved in the pathogenesis, progression, and oncogenic behaviour of human colorectal cancer (Fang and Richardson, 2005; Rezatabar *et al.*, 2019). Nappi *et al.* (2020) and Vidri and Fitzgerald (2020) have stated that the function of enhanced signalling in colorectal cancer through the Ras/Raf/MEK/ERK has become one of the prominent pathway to investigate the cytotoxicity and oncogenic events of xenobiotic such as glycidols in human cells (as provided in *Figure 7*).

CONCLUSION

R- and *S*-glycidol compounds were found less toxic to Vero (normal cells) but it induces cell death in HCT 116 cells. The cytotoxic event of the chemicals has proven that it was due to phosphorylation of ERK ½ proteins that may activate MAPK pathway which activated ROS production and leads to oxidative stress. Furthermore, the docking study showed that the interactions between glycidol and

the 3D-structure of human ERK2 predominantly include hydrogen bonds, Van der Waals interactions and hydrophobic contacts with amino acids, leading to the formation of binding pockets and the stabilisation of protein–ligand complex to support the down regulation event of ERK ½ and p-ERK proteins. In this study, toxicological effects of *R*- and *S*-glycidol were investigated. This finding has shown the similarity of cell death mechanism of treated HCT 116 cells after the exposure of *R*- and *S*-glycidol compounds. However, further investigation should be carried out to elucidate toxicological effects of lower dose *R*-glycidol and *S*-glycidol in *in vivo* study for further safety evaluation.

ACKNOWLEDGEMENT

Laboratory works were carried out at the Centre of Research and Field Service (CRAFT), Universiti Malaysia Terengganu and many thanks to the CRAFT's staff for their contribution in this project. This work was supported by the Ministry of Higher Education Malaysia (FRGS/1/2018/WAB11/UMT/02/1) and UMT for the funding [Fundamental Research Grant Scheme (Vot. 59539)].

REFERENCES

Abbasi, E; Aval, S F; Akbarzadeh, A; Milani, M; Nasrabadi, H T; Joo, S W; Hanifehpour, Y; Nejati-Koshki, K and Pashaei-Asl, R (2014). Dendrimers: Synthesis, applications, and properties. *Nanoscale Res. Letters., 9(1)*: 1–10. DOI: 10.1186/1556-276X-9-247.

Abraham, K; Andres, S; Palavinskas, R; Berg, K; Appel, K E and Lampen, A (2011). Toxicology and risk assessment of acrolein in food. *Mol. Nutr. Food Res., 55(9)*: 1277–1290. DOI: 10.1002/mnfr.201100481.

Akane, H; Shiraki, A; Imatanaka, N; Akahori, Y; Itahashi, M; Ohishi, T; Mitsumori, K and Shibutani, M (2013). Glycidol induces axonopathy by adult-stage exposure and aberration of hippocampal neurogenesis affecting late-stage differentiation by developmental exposure in rats. *Toxicol. Sci., 134(1)*: 140–154. DOI: 10.1093/toxsci/kft092.

Aral, T; Karakaplan, M and Hosgoren, H (2012). Asymmetric organocatalytic efficiency of synthesized chiral beta-amino alcohols in ring-opening of glycidol with phenols. *Catal. Lett., 142(6)*: 794-802. DOI: 10.1007/s10562-012-0814-4.

Arnesano, F; Pannunzio, A; Coluccia, M and Natile, G (2015). Effect of chirality in platinum drugs. *Coordination Chem. Rev., 284*: 286–297. DOI: 10.1016/j.ccr.2014.07.016.

Aurelia, A C; Dobrea, C; Morgovan, C; Arseniu, A M; Rus, L L; Butuca, A; Juncan, A M; Totan, M; Vonica-Tincu, A L; Cormos, G; Muntean, A C; Muresan, M L; Gligor, F G and Frum, A (2020). Applications and limitations of dendrimers in biomedicine. *Molecules., 25(17)*: 3982. DOI: 10.3390/molecules25173982.

Bakhiya, N; Abraham, K; Gürtler, R; Appel, K E and Lampen, A (2011). Toxicological assessment of 3-chloropropane-1, 2-diol and glycidol fatty acid esters in food. *Mol. Nutr. Food Res., 55(4)*: 509–521. DOI: 10.1002/mnfr.201000550.

Bonnier, F; Keating, M E; Wróbel, T P; Majzner, K; Baranska, M; Garcia-Munoz, A; Blanco, A and Byrne, H J (2015). Cell viability assessment using the Alamar blue assay: A comparison of 2D and 3D cell culture models. *Toxicol. In Vitro., 29(1)*: 124–131. DOI: 10.1016/j.tiv.2014.09.014

Brooks, W H; Guida, W C and Daniel, K G (2011). The significance of chirality in drug design and development HHS public access. *Curr. Top. Med. Chem., 11(7)*: 760–770. DOI: 10.2174/156802611795-165098.

Circu, M L and Aw, T Y (2010). Reactive oxygen species, cellular redox systems and apoptosis. *Free Radic. Biol. Med., 48(6)*: 749–762. DOI: 10.1016/j.freeradbiomed.2009.12.022.

Constantinou, C; Papas, A and Constantinou, A I (2008). Vitamin E and cancer: An insight into the anticancer activities of vitamin E isomers and analogs. *Int. J. Cancer., 123(4)*: 739–752. DOI: 10.1002/ijc.23689.

Cregan, I L; Dharmarajan, A M and Fox, S A (2013). Mechanisms of cisplatin-induced cell death in malignant mesothelioma cells: Role of inhibitor of apoptosis proteins (IAPs) and caspases. *Int. J. Oncol., 42(2)*: 444–452. DOI: 10.3892/ijo.2012.1715.

De Luca, A; Maiello, M R; D'Alessio, A; Pergameno, M and Normanno, N (2012). The RAS/RAF/MEK/ERK and the PI3K/AKT signalling pathways: Role in cancer pathogenesis and implications for therapeutic approaches. *Expert Opin. Ther. Targets., 16*: 17–27. DOI: 10.1517/14728222.2011.639361.

EFSA Panel on Contaminants in the Food Chain (CONTAM) (2016). Risks for human health related to the presence of 3- and 2-monochloropropanediol (MCPD), and their fatty acid esters, and glycidyl fatty acid esters in food. *EFSA J., 14(6)*: 04426. DOI: 10.2903/j.efsa.2016.4426.

El Ramy, R; Ould Elhkim, M; Lezmi, S and Poul, J M (2007). Evaluation of the genotoxic potential of 3-monochloropropane-1,2-diol (3-MCPD) and its metabolites, glycidol and β-chlorolactic acid, using the single cell gel/comet assay. *Food Chem. Toxicol., 45(1)*: 41–48. DOI: 10.1016/j.fct.2006.07.014.

Fanali, C; D'Orazio, G; Gentili, A and Fanali, S (2019). Analysis of enantiomers in products of food interest. *Molecules., 24(6)*: 1119. DOI: 10.3390/molecules24061119.

Fang, J Y and Richardson, B C (2005). The MAPK signalling pathways and colorectal cancer. *Lancet Oncol., 6(5)*: 322–327. DOI: 10.1016/S1470-2045(05)70168-6.

Foroumadi, A and Emami, S (2014). Glycidol. *Encyclopedia of Toxicol*. 3rd edition. p. 757-761.

Fu, P P; Xia, Q; Hwang, H M; Ray, P C and Yu, H (2014). Mechanisms of nanotoxicity: Generation of reactive oxygen species. *J. Food Drug Anal., 22(1)*: 64–75. DOI: 10.1016/j.jfda.2014.01.005.

Goh, K M; Wong, Y H; Tan, C P and Nyam, K L (2021). A summary of 2-, 3-MCPD esters and glycidyl ester occurrence during frying and baking processes. *Curr. Res. Food Sci., 4*: 460–469. DOI: 10.1016/j.crfs.2021.07.002.

Hartwig, A; Arand, M; Epe, B; Guth, S; Jahnke, G; Lampen, A; Martus, H J; Monien, B; Rietjens, I M C M; Schmitz-Spanke, S; Schriever-Schwemmer, G; Steinberg, P and Eisenbrand, G (2020). Mode of action-based risk assessment of genotoxic carcinogens. *Arch. Toxicol., 94(6)*: 1787–1877. DOI: 10.1007/s00204-020-02733-2.

Hirata, Y (2021). *Trans*-fatty acids as an enhancer of inflammation and cell death: Molecular basis for their pathological actions. *Biol. Pharm. Bull., 44(10)*: 1349–1356. DOI: 10.1248/bpb.b21-00449.

Inagaki, R; Uchino, K; Shimamura, Y and Masuda, S (2019). Investigation of DNA damage of glycidol and glycidol fatty acid esters using FPG-modified comet assay. *Fundam. Toxicol. Sci., 6(1)*: 9–14. DOI: 10.2131/fts.6.9.

Ji, J; Zhu, P; Sun, C; Sun, J; An, L; Zhang, Y and Sun, X (2017). Pathway of 3-MCPD-induced apoptosis in human embryonic kidney cells. *J. Toxicol. Sci., 42(1)*: 43–52. DOI: 10.2131/jts.42.43.

Kadir, N H A; Rossiter, J T and Gooderham, N J (2009). In vitro toxicology of 2-propenyl and 3-butenyl glucosinolate derivatives. *Toxicol., 262(1)*: 15–16. DOI: 10.1016/j.tox.2009.04.016.

Kim, M J; Park, J; Kim, J; Kim, J Y; An, M J; Shin, G S; Lee, H M; Kim, C H and Kim, J W (2021). Transcriptome analysis reveals $HgCl_2$ induces apoptotic cell death in human lung carcinoma H1299 cells through caspase-3-independent pathway. *Int. J. Mol. Sci., 22(4)*: 2006. DOI: 10.3390/ijms22042006.

Kim, S I; Kim, H J; Lee, H J; Lee, K; Hong, D; Lim, H; Cho, K; Jung, N and Yi, Y W (2016). Application of a non-hazardous vital dye for cell counting with automated cell counters. *Anal. Biochem., 492*: 8–12. DOI: 10.1016/j.ab.2015.09.010.

Lim, S W; Loh, H S; Ting, K N; Bradshaw, T D and Zeenathul, N A (2014). Cytotoxicity and apoptotic activities of alpha-, gamma- and delta-tocotrienol isomers on human cancer cells. *BMC Complement. Altern. Med., 14(1)*: 1–18. DOI: 10.1186/1472-6882-14-469.

Liou, G Y and Storz, P (2010). Reactive oxygen species in cancer. *Free Radic. Res., 44(5)*: 479-496. DOI: 10.3109/10715761003667554.

Liu, P W; Li, C I; Huang, K C; Liu, C S; Chen, H L; Lee, C C; Chiou, Y Y and Chen, R J (2021). 3-MCPD and glycidol coexposure induces systemic toxicity and synergistic nephrotoxicity via NLRP3 inflammasome activation, necroptosis and autophagic cell death. *J. Hazard. Mater., 405*: 124241. DOI: 10.1016/j.jhazmat.2020.124241.

Liu, X; Luo, Q; Rakariyatham, K; Cao, Y; Goulette, T; Liu, X and Xiao, H (2016). Antioxidation and anti-ageing activities of different stereoisomeric astaxanthin *in vitro* and *in vivo*. *J. Funct. Foods., 25*: 50–61. DOI: 10.1016/j.jff.2016.05.009.

Lu, Y; Liu, B; Liu, Y; Yu, X and Cheng, G (2020). Dual effects of active ERK in cancer: A potential target for enhancing radiosensitivity. *Oncol. Lett., 20(2)*: 993–1000. DOI: 10.3892/ol.2020.11684.

Mäder, P and Kattner, L (2020). Sulfoximines as rising stars in modern drug discovery? Current status and perspective on an emerging functional group in medicinal chemistry. *J. Med. Chem., 63(23)*: 14243–14275. DOI: 10.1021/acs.jmedchem.0c00960.

Mahapatra, M and Tysoe, W T (2015). Chemisorptive enantioselectivity of chiral epoxides on tartaric-acid modified Pd (111): Three-point bonding. *Phys. Chem. Chem., 17(7)*: 5450–5458. DOI: 10.1039/c4cp05611f.

Mallepogu, V; Jayasekhar, P B; Doble, M; Suman, B; Nagalakshmamma, V; Chalapathi, P V and Thyagaraju, K (2017). Effects of acrylamide on cervical cancer (HeLa) cells proliferation and few marker enzymes. *Austin J. Biotechnol. Bioeng., 4*: 1087.

Matta, M; Huybrechts, I; Biessy, C; Casagrande, C; Yammine, S; Fournier, A; Olsen, K S; Lukic, M; Gram, I T; Ardanaz, E; Sánchez, M J; Dossus, L; Fortner, R T; Srour, B; Jannasch, F; Schulze, M B; Amiano, P; Agudo, A; Colorado-Yohar, S; Quirós, J R; Tumino, R; Panico, S; Masala, G; Pala, V and Murphy, N (2021). Dietary intake of trans fatty acids and breast cancer risk in 9 European countries. *BMC Med., 19(1)*: 1–11. DOI: 10.1186/s12916-021-01952-3.

McCubrey, J A; Steeman, L; Chappell, W; Abrams, S; Montalto, G; Cervello, M; Nicoletti, F; Fagone, P; Malaponte, G; Mazzarino, M; Candido, S; Libra, M; Basecke, J; Mijatovic, S; Maksimovic-Ivanic, D; Milella, M; Tafuri, A; Cocco, L; Evangelisti, C; Chiarini, F and Martelli, A (2012). Mutations and deregulation of Ras/Raf/MEK/ERK and PI3K/PTEN/Akt/mTOR cascades which alter therapy response. *Oncotarget., 3(9)*: 954–987. DOI: 10.18632/oncotarget.652.

Moreno-Yruela, C; Bæk, M; Monda, F and Olsen, C A (2022). Chiral posttranslational modification to lysine ϵ-amino groups. *Acc. Chem. Res., 55(10)*: 1456–1466. DOI: 10.1021/acs.accounts.2c00115.

Morris, G M; Huey, R; Lindstrom, W; Sanner, M F; Belew, R K; Goodsell, D S and Olson, A J (2009). AutoDock4 and AutoDockTools4: Automated docking with selective receptor flexibility. *J. Comput. Chem., 30(16)*: 2785–2791. DOI: 10.1002/jcc.21256.

Mossoba, M E; Mapa, M S T; Araujo, M; Zhao, Y; Flannery, B; Flynn, T; Sprando, J; Wiesenfeld, P and Sprando, R L (2020). *In vitro* toxicological assessment of free 3-MCPD and select 3-MCPD esters on human proximal tubule HK-2 cells. *Cell Biol. Toxicol., 36(3)*: 209–221. DOI: 10.1007/s10565-019-09498-0.

Nappi, A; Nasti, G; Romano, C; Berretta, M and Ottaiano, A (2020). Metastatic colorectal cancer: Prognostic and predictive factors. *Curr. Med. Chem., 27(17)*: 2779–2791. DOI: 10.2174/0929867326666190620110732.

NavaneethaKrishnan, S; Rosales, J L and Lee, K Y (2019). ROS-mediated cancer cell killing through dietary phytochemicals. *Oxid. Med. Cell. Longev., 2019*: 9051542. DOI: 10.1155/2019/9051542.

Nowak, A; Zakłos-Szyda, M; Żyżelewicz, D; Koszucka, A and Motyl, I (2020). Acrylamide decreases cell viability, and provides oxidative stress, DNA damage, and apoptosis in human colon adenocarcinoma cell line Caco-2. *Molecules., 25(2)*: 368. DOI: 10.3390/molecules25020368.

Obach, R S and Kalgutkar, A S (2010). 1.15—Reactive electrophiles and metabolic activation. *Comprehensive Toxicology.* 2nd edition. p. 309-347. DOI: 10.1016/B978-0-08-046884-6.00115-9.

Ozcagli, E; Alpertunga, B; Fenga, C; Berktas, M; Tsitsimpikou, C; Wilks, M F and Tsatsakis, A M (2016). Effects of 3-monochloropropane-1, 2-diol (3-MCPD) and its metabolites on DNA damage and repair under *in vitro* conditions. *Food Chem. Toxicol., 89*: 1–7. DOI: 10.1016/j.fct.2015.12.027.

Pizzino, G; Irrera, N; Cucinotta, M; Pallio, G; Mannino, F; Arcoraci, V; Squadrito, F; Altavilla, D and Bitto, A (2017). Oxidative stress: Harms and benefits for human health. *Oxid. Med. Cell. Longev., 2017*: 8416763. DOI: 10.1155/2017/8416763.

Redza-Dutordoir, M and Averill-Bates, D A (2016). Activation of apoptosis signalling pathways by reactive oxygen species. *Biochimica et Biophysica Acta (BBA) Molecular Cell Res., 1863*: 2977–2992. DOI: 10.1016/j.bbamcr.2016.09.012.

Rezatabar, S; Karimian, A; Rameshknia, V; Parsian, H; Majidinia, M; Kopi, T A; Bishayee, A; Sadeghinia, A; Yousefi, M; Monirialamdari, M and Yousefi, B (2019). RAS/MAPK signaling functions in oxidative stress, DNA damage response and cancer progression. *J. Cell. Physiol., 234*: 14951–14965. DOI: 10.1002/jcp.28334.

Schilter, B; Scholz, G and Seefelder, W (2011). Fatty acid esters of chloropropanols and related compounds in food: Toxicological aspects. *European J. Lipid Sci. Technol., 113(3)*: 309–313. DOI: 10.1002/ejlt.201000311.

Schumacker, P T (2006). Reactive oxygen species in cancer cells: Live by the sword, die by the sword. *Cancer Cell., 10(3)*: 175–176. DOI: 10.1016/j.ccr.2006.08.015.

Senyildiz, M; Alpertunga, B and Ozden, S (2017). DNA methylation analysis in rat kidney epithelial cells exposed to 3-MCPD and glycidol. *Drug Chem. Toxicol., 40(4)*: 432–439. DOI: 10.1080/01480545.2016.1255951.

Sevim, C; Özkaraca, M; Kara, M; Ulaş, N; Mendil, A S; Margina, D and Tsatsakis, A (2021). Apoptosis is induced by sub-acute exposure to 3-MCPD and glycidol on Wistar Albino rat brain cells. *Environ. Toxicol. and Pharmacology., 87*: 103735. DOI: 10.1016/j.etap.2021.103735.

Sinkala, E; Sollier-Christen, E; Renier, C; Rosàs-Canyelles, E; Che, J; Heirich, K; Duncombe, T A; Vlassakis, J; Yamauchi, K A; Huang, H; Jeffrey, S S and Herr, A E (2017). Profiling protein expression in circulating tumour cells using microfluidic western

blotting. *Nat. Commun., 8*: 14622. DOI: 10.1038/ncomms14622.

Snezhkina, A V; Kudryavtseva, A V; Kardymon, O L; Savvateeva, M V; Melnikova, N V; Krasnov, G S and Dmitriev, A A (2019). ROS generation and antioxidant defense systems in normal and malignant cells. *Oxid. Med. Cell. Longev., 2019*: 6175804. DOI: 0.1155/2019/6175804.

Spungen, J H; MacMahon, S; Leigh, J; Flannery, B; Kim, G; Chirtel, S and Smegal, D (2018). Estimated US infant exposures to 3-MCPD esters and glycidyl esters from consumption of infant formula. *Food Addit. Contam. Part A Chem. Anal., Control Expo. Risk Assess., 35(6)*: 1085–1092. DOI: 10.1080/19440049.2018.1459051.

Takahashi, T; Steinberg, G K and Zhao, H (2012). Phosphorylated MAPK/ERK1/2 may not always represent its kinase activity in a rat model of focal cerebral ischemia with or without ischemic preconditioning. *Neuroscience., 209*: 155–160. DOI: 10.1016/j.neuroscience.2012.02.005.

Tollini, F; Occhetta, A; Broglia, F; Calemma, V; Carminati, S; Storti, G; Sponchioni, M and Moscatelli, D (2022). Influence of pH on the kinetics of hydrolysis reactions: The case of epichlorohydrin and glycidol. *React. Chem. Eng., 7(10)*: 2211–2223. DOI: 10.1039/D2RE00191H.

Vidri, R J and Fitzgerald, T L (2020). GSK-3: An important kinase in colon and pancreatic cancers. *Biochimica et Biophysica Acta (BBA) Molecular Cell Res., 1867(4)*: 118626. DOI: 10.1016/j.bbamcr.2019.118626.

Wróbel, K; Wołowiec, S; Markowicz, J; Wałajtys-Rode, E and Uram, Ł (2022). Synthesis of biotinylated PAMAM G3 dendrimers substituted with R-glycidol and celecoxib/simvastatin as repurposed drugs and evaluation of their increased additive cytotoxicity for cancer cell lines. *Cancers., 14(3)*: 714. DOI: 10.1186/1556-276X-9-247.

Wu, D and Yotnda, P (2015). Production and detection of reactive oxygen species (ROS) in cancers. *J. Vis. Exp., 57*: 3357. DOI: 10.3791/3357.